

Supplementary Information

Synthesis and characterization of a new fluorescent probe for reactive oxygen species.

B. Heyne, Chad Beddie and J.C. Scaiano*

University of Ottawa, Department of Chemistry, 10 Marie Curie, Ottawa, ON, K1N 6N5, Canada

I. Nitrobenzofurazan derivatives.

a) NMR spectra of NBF compound

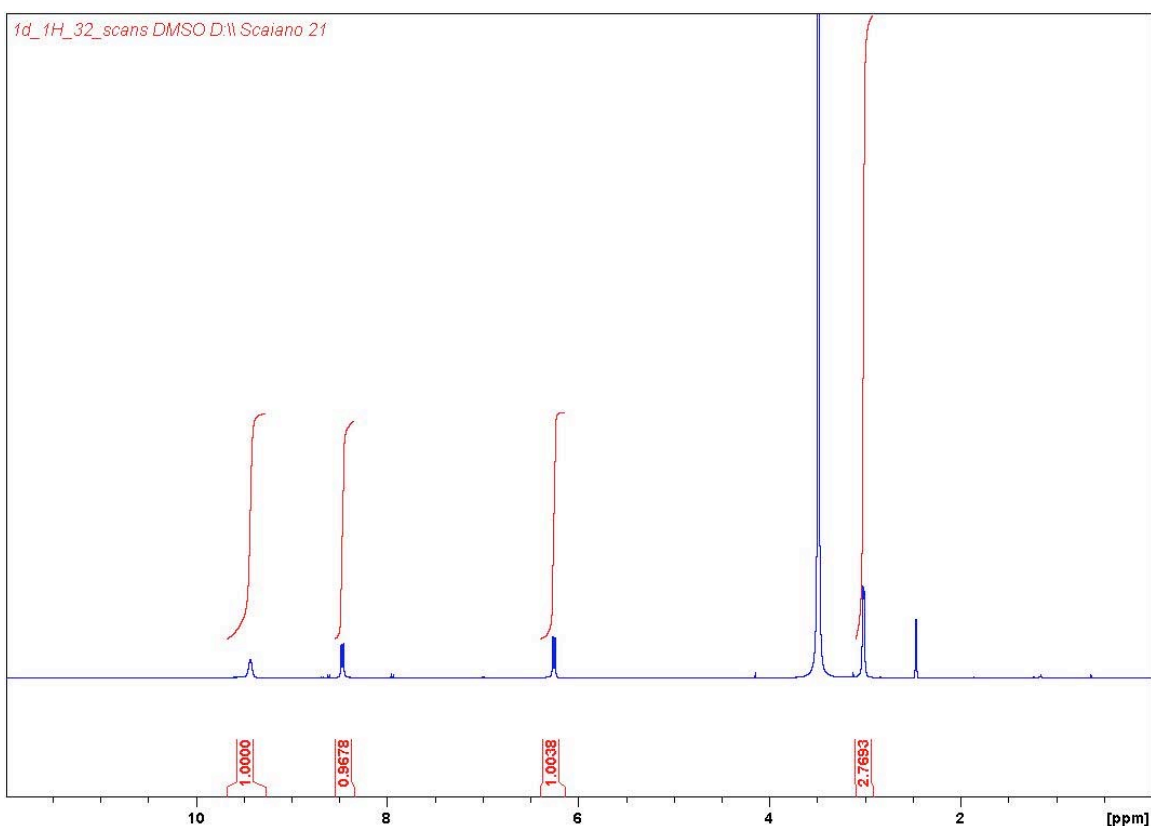


Figure SI 1: ¹H NMR of NBF in DMSO-d₆ at 298 K

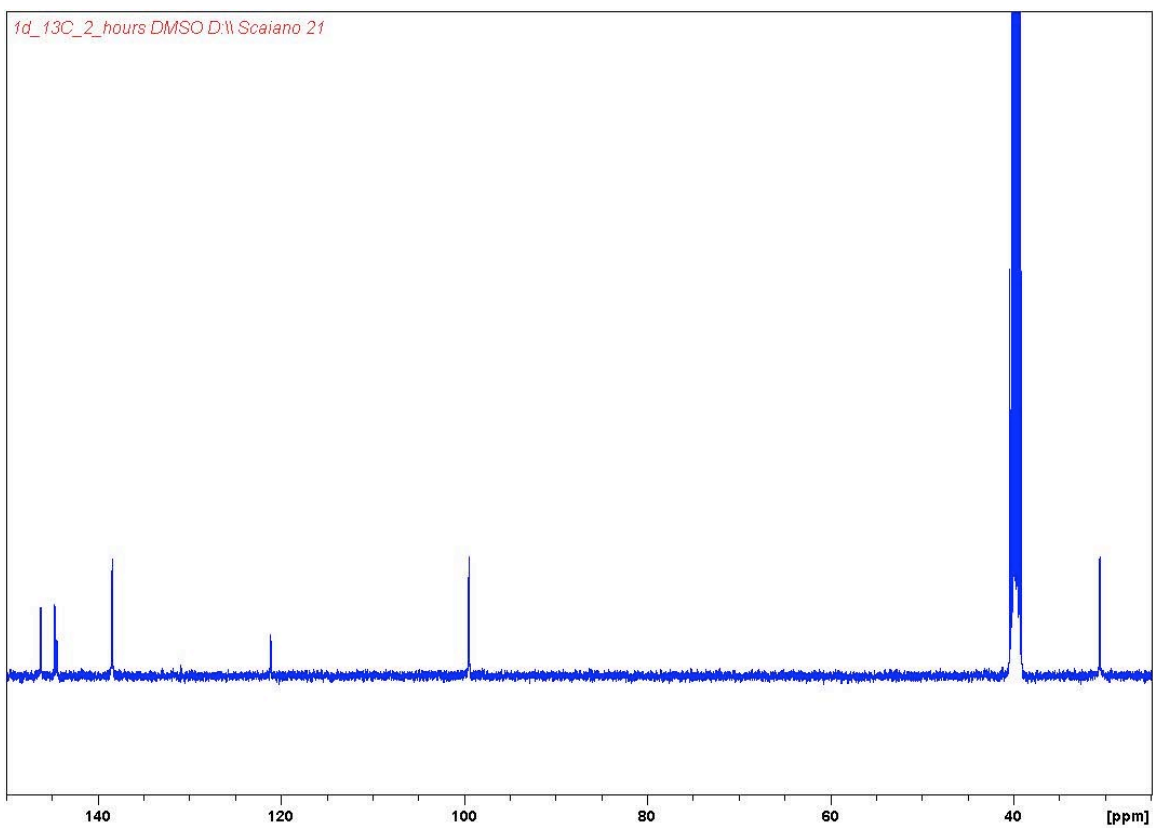


Figure SI 2: ^{13}C NMR of NBF in DMSO- d_6 at 298 K

b) NMR spectra and crystal structure of NBFhd.

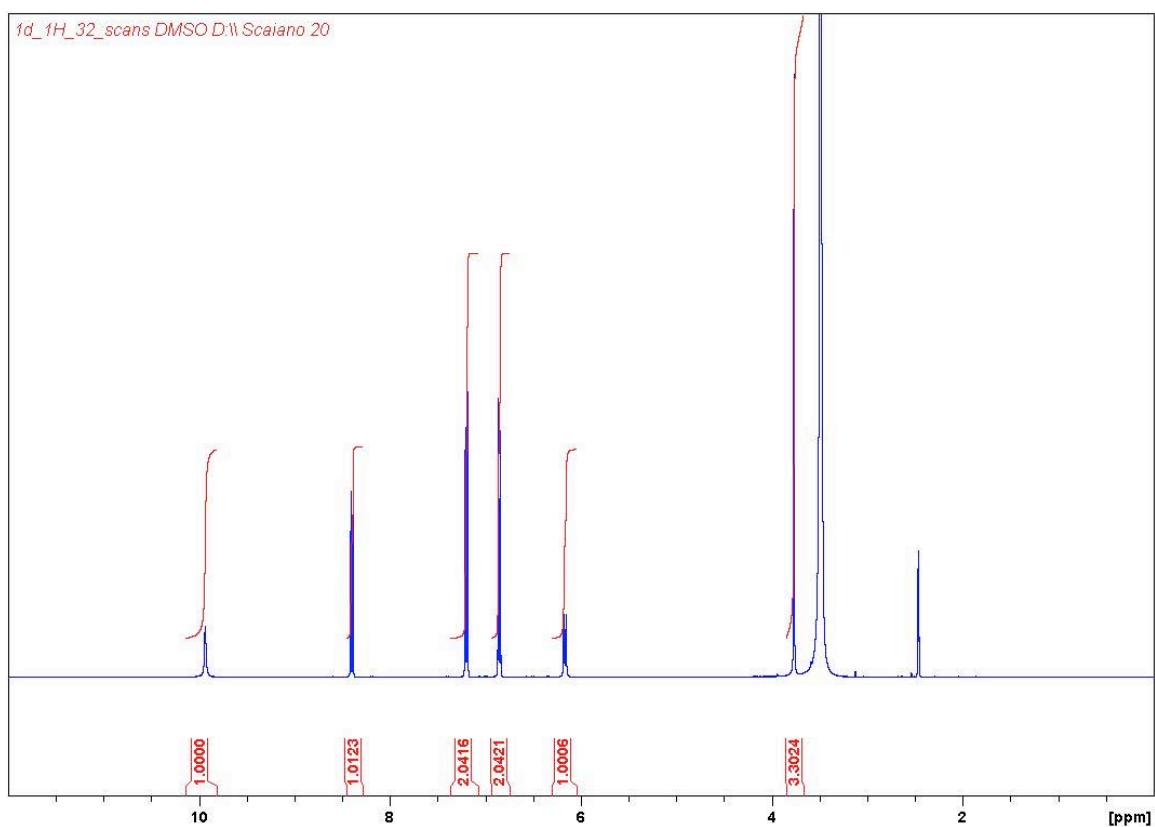


Figure SI 3: ^1H NMR of NBFhd in DMSO-d_6 at 298 K

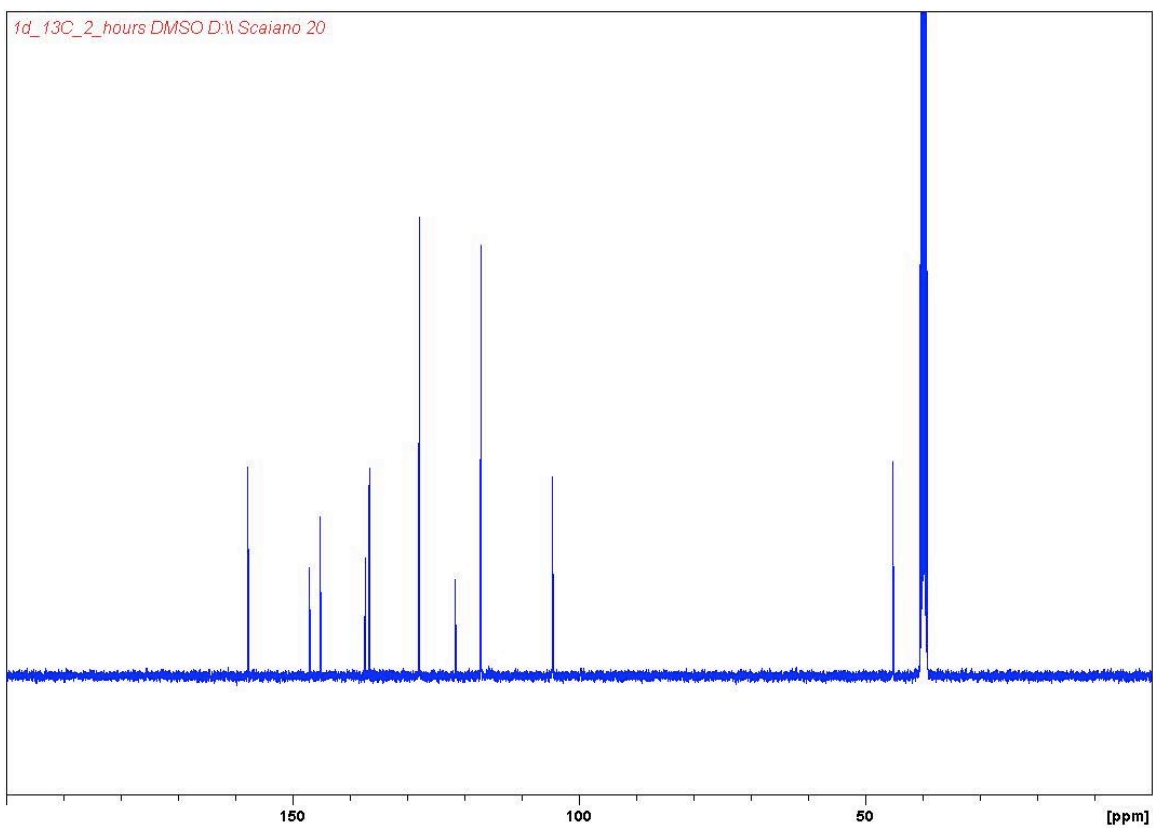


Figure SI 4: ^{13}C NMR of NBFhd in DMSO-d_6 at 298 K

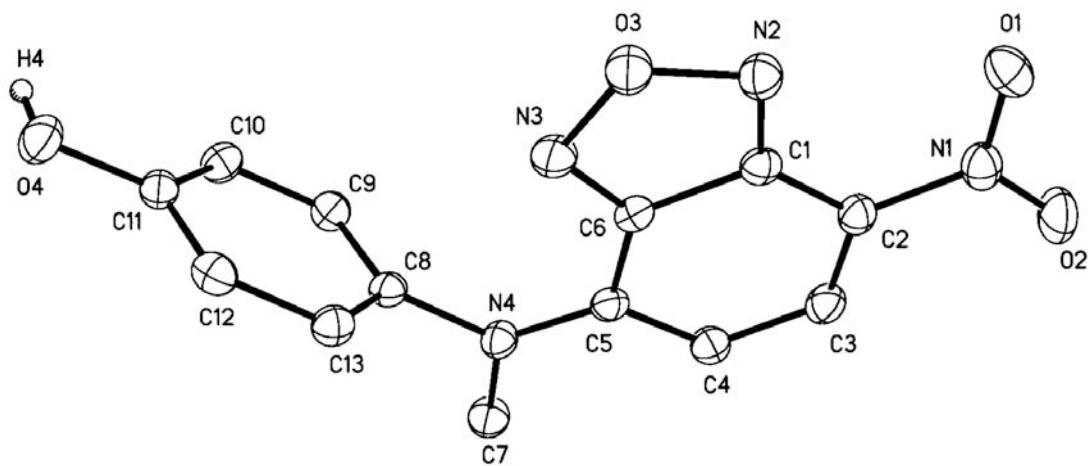


Figure SI 5: ORTEP diagram showing crystal structure of NBFhd

c) Crystallographic data for NBFhd

Empirical formula	C13 H10 N4 O4
Formula weight	286.25
Temperature	200 (2) K
Wavelength	0.71073 Å
Crystal system, space group	Monoclinic, P2(1)/n
Unit cell dimensions	a=8.5125 (15) Å α=90° b=14.863 (3) Å β=92.917 (3)° c=9.7571 (17) Å γ=90°
Volume	1232.9 (4) Å ³
Z, Calculated density	4, 1.542 Mg/m ³
Absorption coefficient	0.118 mm ⁻¹
F(000)	592
Crystal size	0.2 x 0.15 x 0.15 mm
Theta range for data collection	2.5 to 24.73 deg.
Limiting indices	-9<=h<=10, -17<=k<=17, -11<=l<=11
Reflections collected / unique	8836 / 2048 [R(int) = 0.0419]
Completeness to theta = 24.73	97.4%
Absorption correction	Semi-empirical from equivalents
Max. and min. transmission	0.9825 and 0.9768
Refinement method	Full-matrix least-squares on F ²
Data / restraints / parameters	2048 / 0 / 192
Goodness-of-fit on F ²	1.005
Final R indices [I>2sigma (I)]	R1 = 0.0353, wR2 = 0.0830
R indices (all data)	R1 = 0.0656, wR2 = 0.0960
Largest diff. peak and hole	0.144 and -0.134 e.Å ³

Definition of R indices: $R1 = \sum(F_0 - F_c) / \sum(F_0)$; $wR2 = [\sum[w(F_0^2 - F_c^2)^2] / \sum[w(F_0^2)^2]]^{1/2}$

II. Chromatographic analysis of the interaction between peroxy radical and NBFhd.

Released of NBF from the interaction between peroxy radical and NBFhd.

The interaction between peroxy radical produced by the thermal decomposition of AAPH at 40°C and NBFhd was performed by HPLC (Jasco) with fluorescence detection (model FP-1520). Briefly, a solution of NBFhd (5×10^{-6} M) dissolved in PBS (15 mM $\text{NaH}_2\text{PO}_4/\text{K}_2\text{HPO}_4$, pH 7.4) in presence of AAPH (5×10^{-3} M) was kept under air at 40°C in a water bath. The mixture was then injected without any treatment on a C-18 reverse phase column (Zorbax, SB-C18 4.6×250 mm, Agilent). An isocratic elution with a mixture of water and acetonitrile (30:70) was realized at a flow rate of 1 ml/min for 10 min. The excitation wavelength of the fluorescence detector was set at 468 nm, while the emission wavelength was 550 nm.

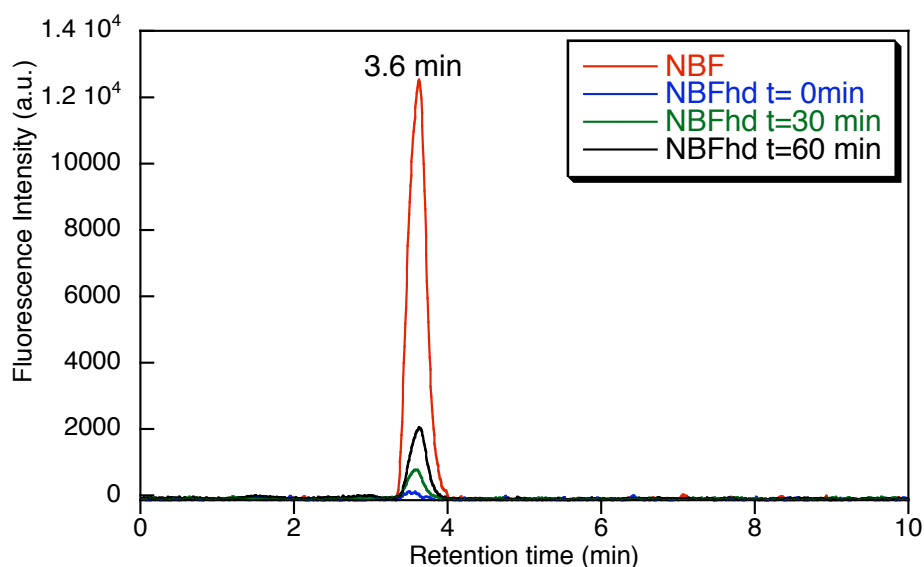


Figure SI 6: HPLC chromatograph with fluorescence detection of a solution of NBF 5×10^{-6} M and NBFhd 5×10^{-6} M incubated with AAPH 5×10^{-3} M in PBS pH for 30 and 60 min.

Characterization of the by-products resulting from the interaction between peroxy radical and NBFhd.

The interaction between peroxy radical produced by the thermal decomposition of AAPH at 40°C and NBFhd was also performed by GC/MS. A solution of NBFhd (10^{-4} M) dissolved in PBS (15 mM $\text{NaH}_2\text{PO}_4/\text{K}_2\text{HPO}_4$, pH 7.4) in presence of AAPH (10^{-1} M) was kept under air at 40°C for 0 and 30 min in a water bath. The sample was acidified by addition of 20 μl HCl (8 mM) then extracted in 1ml of chloroform. The extracted sample

was injected without further purification on the column (Agilent HP-5MS, 0.25mm*30m*0.25um) of the GC/MS chromatogram (Agilent technologies). The injector temperature was set at 250°C. The temperature program began at 50°C (for 10 min) and was increased up to 280°C (for 10 min) at a rate of 10°C/min. The temperature of the MS detector (Agilent, model 5973) was set at 150°C.

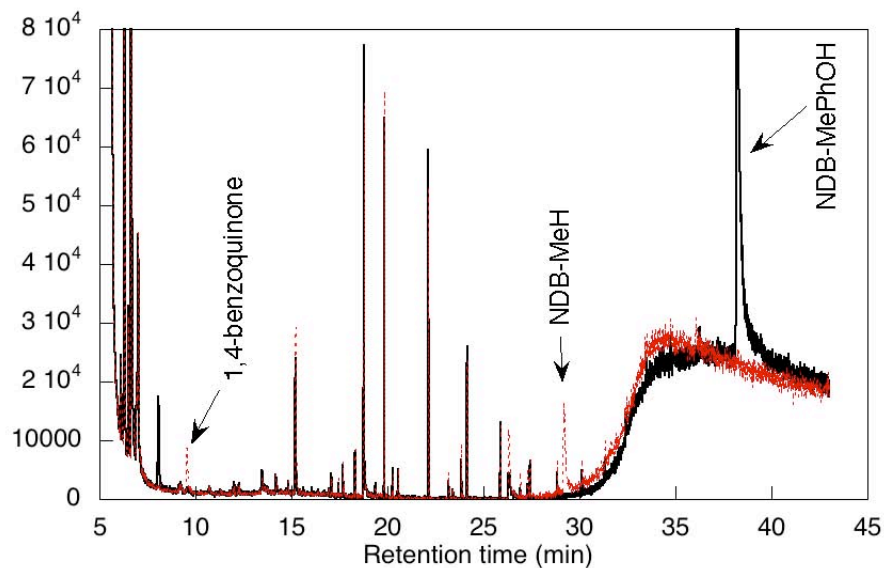


Figure SI 7: GC chromatogram of a solution of NBFhd (10^{-4} M) incubated in PBS pH 7.4 in presence of AAPH (10^{-1} M) at 40°C for 0 min (black trace) and 30 min (red trace), respectively.

III. Calculated Structures.

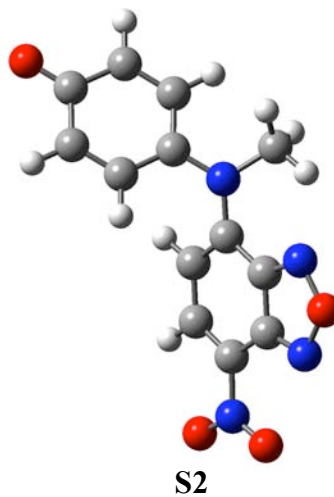
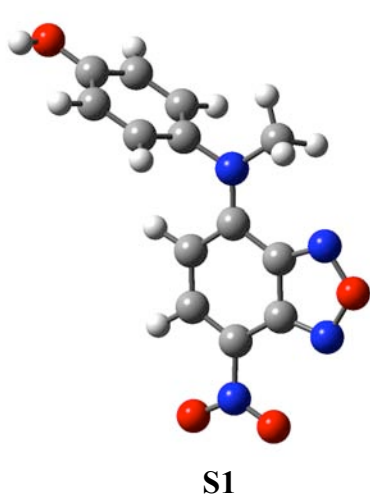
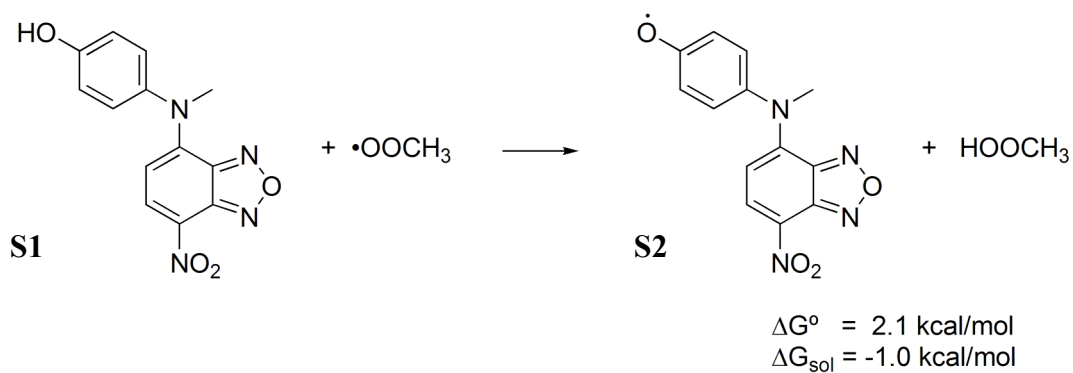
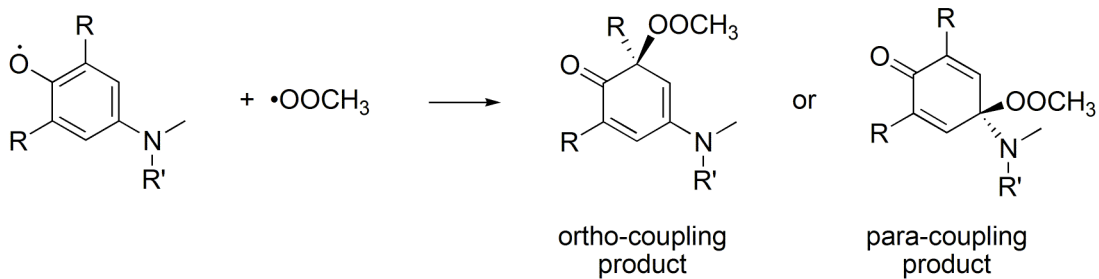
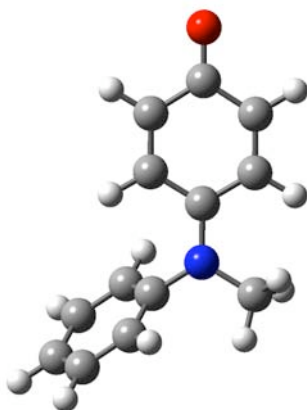


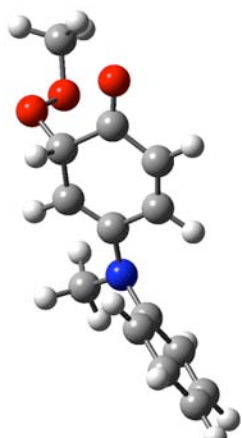
Figure SI 8: Calculated structures of the molecules in Figure 5.



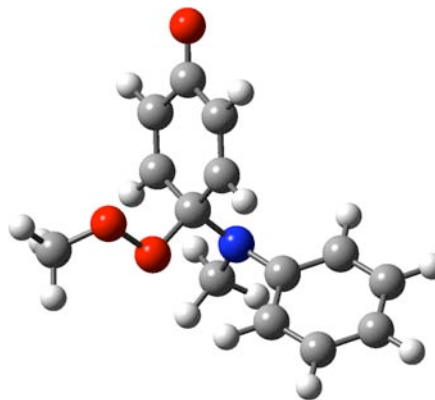
Model 2: R = H, R' = phenyl
 Model 3: R = CH₃, R' = phenyl



**Model 2
Initial radical**

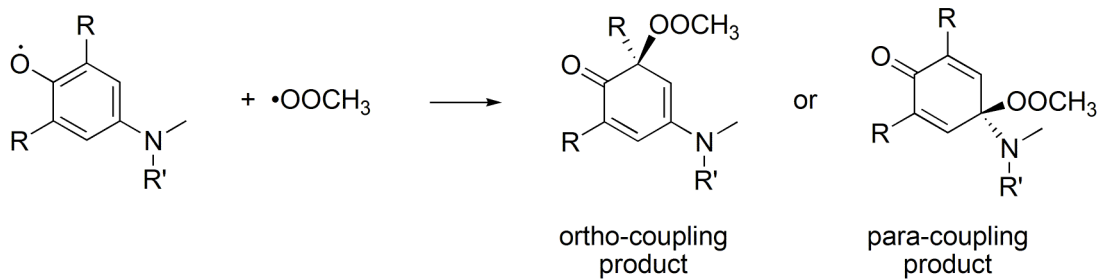


**Model 2
Ortho coupling product**



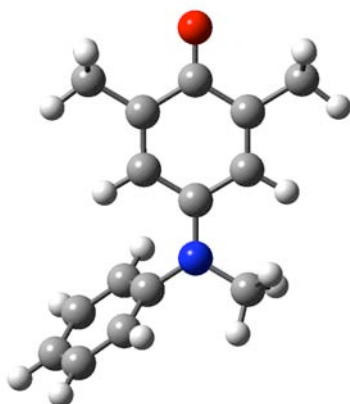
**Model 2
Para coupling product**

Figure SI 9: Calculated structures the initial radical and the ortho and para coupling products for Model 2 described in Figure 7 in the article.

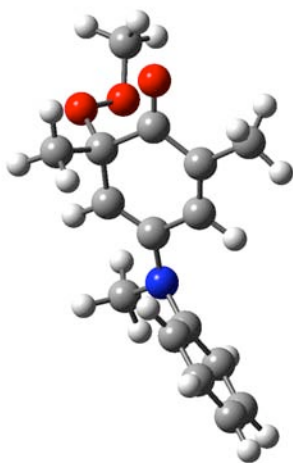


Model 2: R = H, R' = phenyl

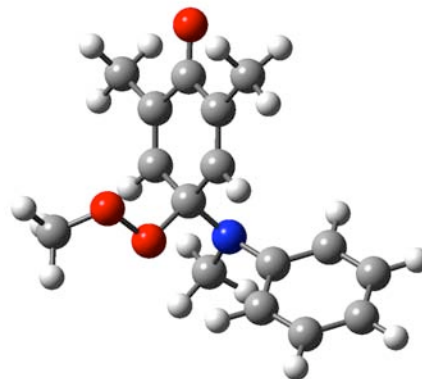
Model 3: R = CH₃, R' = phenyl



**Model 3
Initial Radical**



**Model 3
Ortho-coupling
product**



**Model 3
Para-coupling
product**

Figure SI 10: Calculated structures the initial radical and the ortho and para coupling products for the Model 3 described in Figure 7 in the article.